Dipolar broadening in pulsed NMR in domain walls

Mary Beth Stearns
Scientific Research Staff, Ford Motor Company, Dearborn, Michigan 48121
(Received 14 April 1975)

Calculations are made of the pulsed NMR line shapes due to dipolar shifts at nuclei in the first three neighbor shells surrounding a solute atom. We find that the line shapes are very dependent on the angles through which the nuclei are turned and discuss the optimum operating conditions to observe dipolar broadening. Measured dipolar shifts in ordered FeSi alloys are shown to agree excellently with calculated shifts. It is observed that $4d$ and $5d$ transition solute atoms give rise to anomalously broadened lines.

I. INTRODUCTION

The quality of pulsed NMR spectra of Fe alloys has become so good in recent years that dipolar broadening must be taken into account in order to analyze the spectra properly. The effects of domain-wall dipolar shifts on the behavior of the NMR signal have been discussed by Murray and Marshall[1] (MM) for the case in which the NMR signal was assumed to be proportional to the square of the enhancement factor ϵ. In reality, the NMR signal strength and enhancement-factor variation are much more complex than they assumed, and we derive the more realistic behavior in Sec. II. There we see that the shape of the dipolar broadening depends on the angles through which the nuclear spins are turned. In Sec. III we compare the measured dipolar splittings obtained in NMR[2] and Mössbauer[3] experiments with the calculated values. We show that for the case of Si, a small nontransition-element solute atom, there appear to be no moment or spacial distortions of the host lattice upon substituting a Si atom for an Fe atom. On the other hand, it appears that appreciable distortions, greater than the dipolar broadening, are present when $4d$ or $5d$ transition-series elements replace a host Fe atom.

II. CALCULATION OF BROADENING FOR Fe ALLOYS

At purely cubic sites there are no dipolar effects. However, removing the cubic symmetry by introducing solute atoms gives rise to dipolar shifts in the Fe atoms near the solute atom. In powdered Fe alloys the NMR signal originates overwhelmingly in the domain walls. This arises because the enhancement factor at the center of the walls is about a factor of 30 greater than in the domains, and the spread in frequencies in the domains is very large owing to the variation in demagnetizing factors. Since the magnetization direction varies in the domain wall, the dipolar shifts of Fe atoms near a solute atom depends on its position in the wall.

Let z be the direction of magnetization in a domain and x be the direction perpendicular to the domain wall. It is well known[4] that, from considering the wall energy per unit area arising from anisotropy, K, and exchange, A, energy densities, the variation of the angle φ between the direction of magnetization in the wall and the domain is given by

$$\frac{d\varphi}{dx} = \frac{1}{\delta \sin\varphi \cos\varphi} \ , \tag{1}$$

where δ is a characteristic length of $\simeq 230$ Å for Fe and is given by $(A/K)^{1/2}$. Taking the origin at the center of a 90° wall (i.e., $x=0$ and $\varphi = 45°$), the enhancement factor ϵ varies as $\operatorname{sech} x$, where x is measured in units of δ. A 180° wall can be considered to be two back-to-back 90° walls.

We have previously developed the model of a domain wall in which the wall is represented by a vibrating drumhead.[5] This model describes very well all of the observed behavioral aspects (shape and strength of free induction decays and echoes, relaxation times) of pulsed NMR in Fe and its alloys. The enhancement factor was seen to depend on the radial position of the nucleus in the drumhead, measured in units of the radius of the drumhead r_0 and the maximum displacement h at the center of the drumhead. Thus the enhancement factor is given by

$$\epsilon = \epsilon_0 \operatorname{sech} x(1 - r^2)h \ , \tag{2}$$

where ϵ_0 is the maximum enhancement factor at the center of a 90° wall. If the sample is excited with two rf pulses of magnitude B_1 (in the sample) and frequency ω, then the echo height is given by[5]

$$\begin{aligned} \mathcal{E}(\omega, B_1, \tau_1, \tau_2) \simeq \Big[\Big(\int_0^\infty \int_0^1 \epsilon \sin^3\theta \sin b\tau_1 \sin^2 \tfrac{1}{2}(b\tau_2) \\ \times p(h) r \sin\eta \, d\eta \, dx \, dr \, dh \Big)^2 \\ + \Big(\int_0^\infty \int_0^1 \epsilon \sin^3\theta \cos\theta (1 - \cos b\tau_1) \sin^2 \tfrac{1}{2}(b\tau_2) \\ \times p(h) r \sin\eta \, d\eta \, dx \, dr \, dh \Big)^2 \Big]^{1/2} \ , \end{aligned} \tag{3}$$

where η is the angle between the direction of the rf field and the magnetization in the domain. We must average over this angle since the magnetization directions in the powdered sample are random. $p(h)$ is the probability distribution of the maximum displacements; for reasons given in Ref. 5, it is taken as constant. As usual, θ and b are defined by

$$\tan\theta = \epsilon\gamma B_1 \cos\eta/\Delta\omega_n \ , \tag{4}$$

$$b = (\Delta\omega_n^2 + \epsilon\gamma B_1 \cos\eta)^{1/2} \ , \tag{5}$$

where γ is the nuclear gyromagnetic ratio, $\Delta\omega_n = \omega - \omega_n$, and ω_n is the resonance frequency of the nuclei. We will shortly consider the variation of $g(\omega)$ through the wall due to dipolar fields. For computation purposes, since $h(1-r^2)\cos\eta$ always occur in that combination, we can find a joint distribution function and reduce the quadruple integral in Eq. (3) to a double integral. This is done by letting

$$z = h(1-r^2)\cos\eta \ ; \tag{6}$$

we then find that

$$p(z) = \tfrac{1}{2}\ln^2(1/z) \ \text{ for } 0 \le z \le 1 \ . \tag{7}$$

Equation (3) thus becomes

$$g(\omega) \simeq \Bigg[\Bigg(\int_0^\infty \int_0^1 \sin^3\theta \sin b\tau_1 \sin^2\tfrac{1}{2}(b\tau_2) \times z \ \mathrm{sech}\, x \ln^2(1/z)\, dx\, dz \Bigg)^2 + \Bigg(\int_0^\infty \int_0^1 \sin^3\theta \cos\theta (1-\cos b\tau_1) \sin^2\tfrac{1}{2}(b\tau_2) \times z \ \mathrm{sech}\, x \ln^2(1/z)\, dx\, dz \Bigg)^2 \Bigg]^{1/2} \ . \tag{8}$$

For given B_1, τ_1, and τ_2, this can be easily evaluated on a computer. It is worth noting that Eq. (8) does not take into account the frequency spread of the exciting rf pulse due to the finite length of the rf pulses. This could be introduced by putting in this frequency distribution and averaging over these frequencies, as was found necessary to do in order to explain the origin of single-pulse echoes,[6] which are so prominent in NMR measurements on Co. In Eq. (8) we also have not taken into account the "natural" linewidth of the NMR resonance due to imperfection in the Fe lattice and relaxation processes. Again, this could be done by putting in its frequency distribution and averaging with another integration over ω_n. Usually this is not necessary, and the results we obtain here would be changed little by these extra integrations.

A. Evaluation of ω_n in the domain wall

We evaluate the frequency dependence of the nuclei with position in the wall in the same manner as Ref. 1. The only difference is that here we want the frequency shift as a function of x rather than φ, so that we can substitute it directly into Eqs. (4) and (5), which are then used in evaluating Eq. (8). The dipolar shift caused at a nucleus by a solute atom with moment μ_x which is a distance r_i away is given by

$$H_i = \mu_x [1 - 3(\vec{\mathrm{M}} \cdot \vec{\mathrm{R}})^2]/r_i^3 \ , \tag{9}$$

where $\vec{\mathrm{R}}$ is the unit vector in the direction of the solute atom and $\vec{\mathrm{M}}$ is the magnetization direction in the wall, given by

$$\vec{\mathrm{M}} = \sin\varphi\, \vec{\mathrm{j}} + \cos\varphi\, \vec{\mathrm{k}} \ . \tag{10}$$

1. First-nearest neighbors (N1)

The unit vectors of the $N1$ sites are given by

$$\vec{\mathrm{R}} = \pm(1/\sqrt{3})(\vec{\mathrm{i}} + \vec{\mathrm{j}} + \vec{\mathrm{k}}); \ \pm(1/\sqrt{3})(-\vec{\mathrm{i}} + \vec{\mathrm{j}} + \vec{\mathrm{k}}) \ ; \ \pm(1/\sqrt{3})(\vec{\mathrm{i}} - \vec{\mathrm{j}} + \vec{\mathrm{k}}); \ \pm(1/\sqrt{3})(i + j - k) \ . \tag{11}$$

From Eq. (9) we find that four of the $N1$ sites would cause a shift of $2\Delta_1\cos\varphi$, and four would cause a shift of $-2\Delta_1\cos\varphi$, where $\Delta_1 = \mu_x/r_1^3$. Since from Eq. (1) $\tan\varphi = e^{-x}$ (x in units of δ), we find for the frequency shifts at position x

$$\begin{aligned} &4 \text{ sites}, \quad \Delta_1 \,\mathrm{sech}\, x \ , \\ &4 \text{ sites}, \quad -\Delta_1 \,\mathrm{sech}\, x \ , \end{aligned} \tag{12}$$

where Δ_1 is now taken in frequency units. Thus $\omega_n = \omega_0 \pm \Delta_1 \,\mathrm{sech}\, x$, where ω_0 is the center resonance frequency in pure Fe. We have evaluated Eq. (8) for these values of ω_n (with their proper weightings) for a variety of values of maximum turning angle $\alpha_1 = \gamma\epsilon_0 B_1 \tau_1$. This is the angle through which nuclei at the center of the wall are turned by the first pulse. ϵ_0 is the maximum enhancement factor of the nuclei at the center of the wall. It is determined experimentally for any particular Fe alloy.[5] The echo height is a maximum at $\alpha_1 \simeq 5$ rad and $\tau_2 \simeq 2\tau_1$. Some calculated frequency distributions $g(\omega)$ are shown in Figs. 1 and 2. We show two types of plots. One, for a fixed Δ_1, emphasizes how the spectra change with different turning angles of the rf pulses. The other shows how the spectra vary with Δ_1 for the optimum fixed turning angles of $\alpha_1 = 5$ rad, $\alpha_2 = 10$ rad. For a NMR signal which only varies as $\epsilon^2 \simeq \mathrm{sech}^2 x$, MM found a frequency distribution which was strongly peaked at $\Delta\omega_n = \pm\Delta_1$. Figure 1 shows $g(\omega)$ as a function of $\Delta\omega t_1$ ($\Delta\omega = \omega - \omega_0$) for the case of very large dipolar splitting such that $D = 2\pi\Delta_1 t_1 = 4$. We see that for reasonable turning angles the splitting is slightly less than $2\Delta_1$ and approaches $2\Delta_1$ as $\alpha_1 \to 0$. For large turning angles (e.g., see $\alpha_1 = 4\pi$), the spectra become very complex and it is difficult to separate the turning-angle effects from the dipolar structure. The oscillations seen in

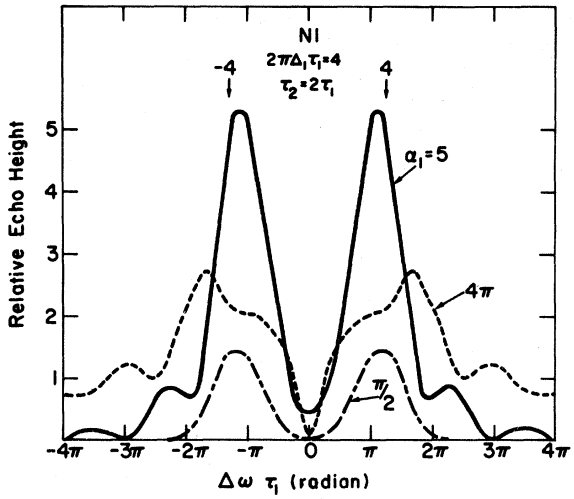

FIG. 1. Variation of line shape with turning angle at nearest neighbors to a solute atom. The dipolar shift $2\pi\Delta_1\tau_1$ is taken as 4.

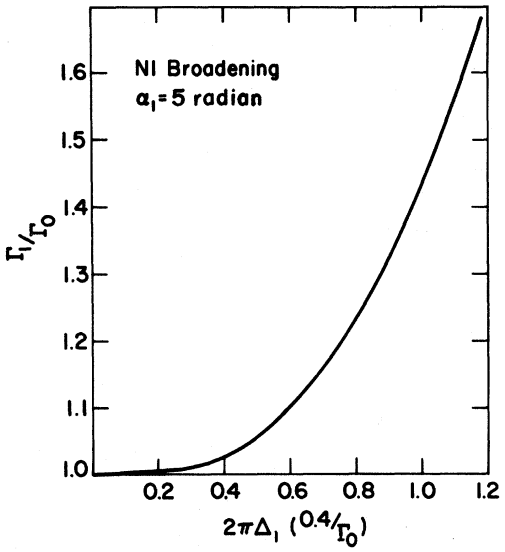

FIG. 3. Calculated ratio of $N1$ linewidth Γ_1 to main linewidth Γ_0 as a function of $N1$ dipolar shift. The linewidths are the full widths at half-height measured in MHz.

Figs. 1 and 2 due to turning-angle effects are usually washed out from other broadening effects in alloys. The correct relative echo heights are shown in Fig. 1. Thus it is clear that the best operating condition for seeing the $N1$ dipolar splitting is at turning angles $\alpha_1 \simeq 5$ rad, or less if the signal strength is strong enough. Figure 2 shows the behavior of the $N1$ dipolar splitting for a first turning angle of 5 rad as a function of the dipolar shift $D = 2\pi\Delta_1 t_1$. For the usual dipolar shifts in Fe alloys, D is about 1; so we expect to see only a broadening of the spectrum due to $N1$ effects. This has been observed in ordered FeSi alloys, and is discussed in Sec. III.

In Fig. 3 we give the calculated broadening of the $N1$ line Γ_1 compared to the main linewidth Γ_0 as a function of the dipolar shift for $\alpha_1 = 5$ rad and $\alpha_2 = 10$ rad. The abscissa is taken as $2\pi\Delta_1(0.4/\Gamma_0)$. This is because the full width at half-height, $\Delta\nu_{1/2}$, due to turning angle effects, occurs at $2\pi\Delta\nu_{1/2}\tau_1 = 0.8\pi$ (see Fig. 2). We then assumed that in practice the smallest value of τ_1 is used that gives no observable broadening of the main line. This then corresponds to $\tau_1 = 0.4/\Gamma_0$, and D becomes $2\pi\Delta_1 \times (0.4/\Gamma_0)$. In reality, one could measure the spectrum with larger values of τ_1, but to get the optimum turning angle this would require reducing B_1. However, under usual operating conditions the signal strength increases with larger B_1; so increasing τ_1 (and reducing B_1 to hold α_1 constant) will result in a poorer signal-to-noise ratio.

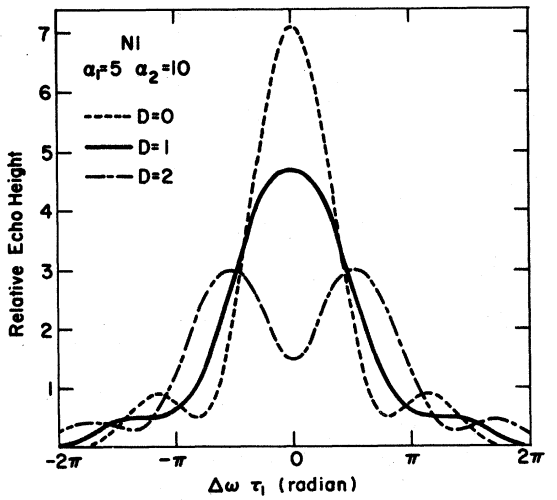

FIG. 2. Variation of line shape with dipolar shift at nearest neighbors to a solute atom. $D = 2\pi\Delta_1\tau_1$.

2. Second-nearest neighbors (N2)

The unit vectors of the $N2$ sites are given by

$$\vec{R} = \pm\vec{i};\ \pm\vec{j};\ \pm\vec{k}\ . \tag{13}$$

From Eq. (9), we find the following shifts;

$$\begin{aligned} &2 \text{ sites},\ \Delta_2; \\ &2 \text{ sites},\ \Delta_2(1-3\cos^2\varphi) \text{ or } \Delta_2(e^{-2x}-2)/(1+e^{-2x}), \\ &2 \text{ sites},\ \Delta_2(1-3\sin^2\varphi) \text{ or } \Delta_2(1-2e^{-2x})/(1+e^{-2x}), \end{aligned} \tag{14}$$

where $\Delta_2 = \mu_x/r_2^3$. We use these values in evaluating Eq. (8). For their signal variations, $\sim g^2$, MM obtained a δ function at Δ_2 with a flat probability distribution between $-2\Delta_2$ and Δ_2. We see in Fig. 4 that the spectra are somewhat like this for very small turning angles, but become quite different for higher turning angles, approaching a peak at

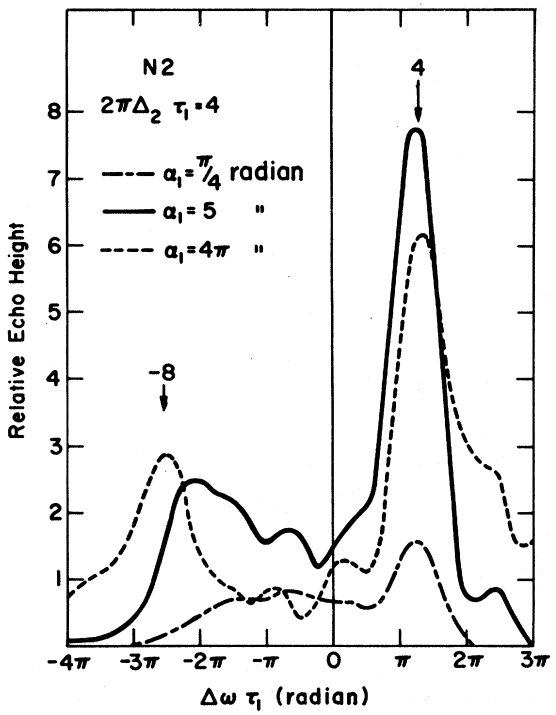

FIG. 4. Variation of line shape with turning angle at second-nearest neighbors to a solute atom for dipolar shift of $2\pi\Delta_2\tau_1=4$.

Δ_2 with $\frac{2}{3}$ the intensity and a peak at $-2\Delta_2$ with $\frac{1}{3}$ the intensity, as would be seen in the domains. This occurs because at large turning angles the signals from the nuclei at the center of the wall tend to get averaged out and mainly those at the edges of the wall contribute to the NMR signal. In Fig. 5 we show the $N2$ dipolar broadening for various values of D and $\alpha_1=5$ rad, $\alpha_2=10$ rad. It is clear from Figs. 4 and 5 that large turning angles give the best operating conditions to observe the dipolar splitting due to $N2$. For instance, a turning angle α_1 of about 10 rad is probably about optimum. The correct relative intensities are shown in Figs. 4 and 5; so not much intensity is lost in operating at $\alpha_1\sim 10$ rad. Notice that the optimum conditions for observing the dipolar broadening are different for $N1$ and $N2$, although $\alpha_1\simeq 5$ rad is a good compromise for both. For Fe and its alloys, the value of $2\pi\Delta_2\tau_1$ corresponds to values of $D\simeq 1$. We have clearly seen $N2$ broadening in ordered FeSi alloys. This is discussed in Sec. III.

3. *Third-nearest neighbors (N3)*

The unit vectors for the $N3$ sites are

$$\vec{R}=\pm(1/\sqrt{2})(\vec{i}+\vec{j});\quad \pm(1/\sqrt{2})(\vec{j}+\vec{k});\quad \pm(1/\sqrt{2})(\vec{i}+\vec{k});$$
$$\pm(1/\sqrt{2})(\vec{i}-\vec{j});\quad \pm(1/\sqrt{2})(\vec{j}-\vec{k});\quad \pm(1/\sqrt{2})(\vec{i}-\vec{k})\,. \tag{15}$$

From Eq. (9) we find the following shifts:

$$\begin{aligned}
&4\text{ sites},\ \Delta_3(1-\tfrac{3}{2}\cos^2\varphi)\\
&\quad\text{or }\Delta_3(e^{-2x}-\tfrac{1}{2})/(1+e^{-2x});\\
&4\text{ sites},\ \Delta_3(1-\tfrac{3}{2}\sin^2\varphi)\\
&\quad\text{or }\Delta_3(1-\tfrac{1}{2}e^{-2x})/(1+e^{-2x});\\
&2\text{ sites},\ -\Delta_3(\tfrac{1}{2}+3\cos\varphi\sin\varphi)\\
&\quad\text{or }-\Delta_3|(1+3\,\mathrm{sech}\,x);\\
&2\text{ sites},\ -\Delta_3(\tfrac{1}{2}-3\cos\varphi\sin\varphi)\\
&\quad\text{or }-\Delta_3'(1-3\,\mathrm{sech}\,x)\ ,
\end{aligned} \tag{16}$$

where $\Delta_3=\mu_x/r_3^3$. We use these values to evaluate Eq. (8). In Fig. 6 we show the $N3$ dipolar broadening for various values of D at a first turning angle of 5 rad. For an Fe moment typical values of D are ~ 0.5; so in some cases the $N3$ broadening may be discernible ($\sim 10\%$). In Fig. 7 we show the broadening Γ_3/Γ_0 for full widths at half-height as a function of $2\pi\Delta_3(0.4/\Gamma_0)$. All widths are to be

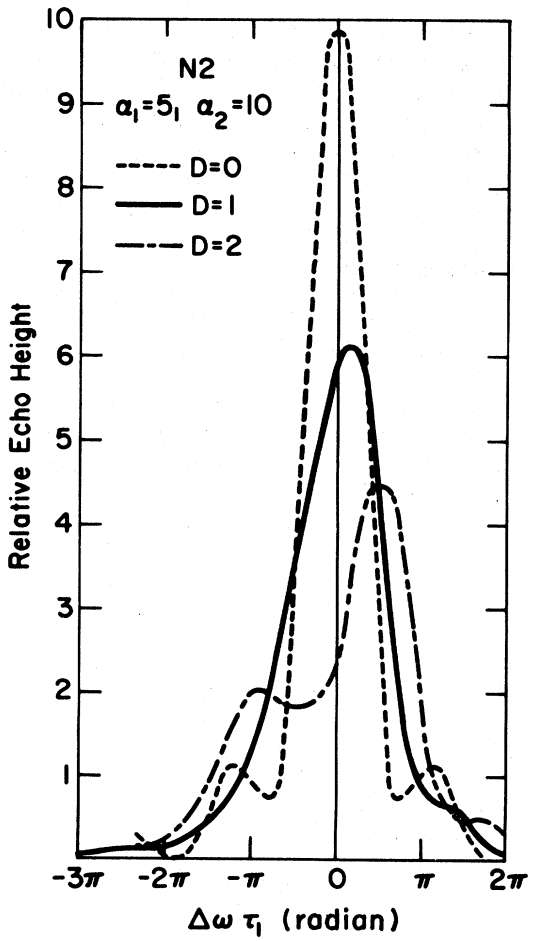

FIG. 5. Variation of line shape with dipolar shift at the second-nearest neighbors to a solute atom. $D=2\pi\Delta_2\tau_1$.

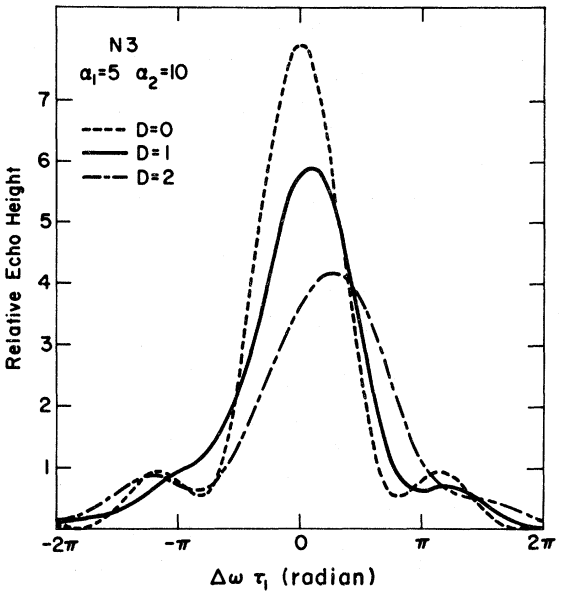

FIG. 6. Variation of line shape with dipolar shift at the third-nearest neighbors to a solute atom. $D=2\pi\Delta_3\tau_1$.

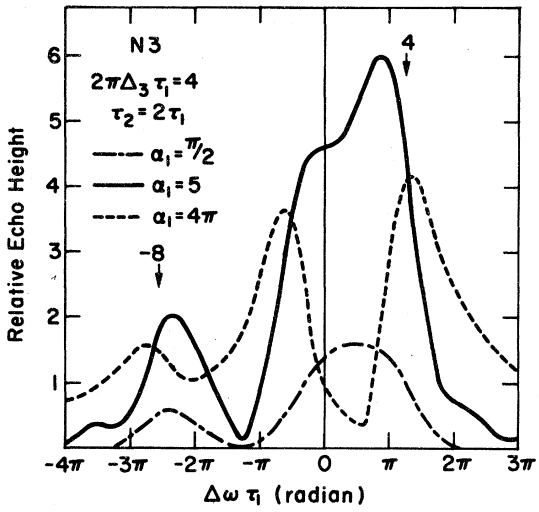

FIG. 8. Variation of line shape with turning angle at the third-nearest neighbors to a solute atom for a dipolar shift of $2\pi\Delta_3\tau_1=4$.

measured in MHz. In Fig. 8 we show how the $N3$ dipolar broadening varies for different turning angles for a very large dipolar shift of $2\pi\Delta_3\tau_1=4$.

III. COMPARISON WITH EXPERIMENT

Attempts to measure dipolar shifts have been made by Cranshaw *et al.*[3] with a very clever Mössbauer-type experiment on single-crystal alloys. In Mössbauer experiments mainly the nuclei in the domains are measured, since there are many more of them and there is no such thing as an enhancement factor. To obtain a different type of spectra, the direction of magnetization in a thin foil was varied by applying an external field. Spectra were taken with the field applied in the [100] and [111] directions. The difference spectrum was then used to obtain the dipolar shifts. The difficulty with the Mössbauer technique for such measurements is that the inherent linewidth for Fe (~16 kG) is much larger than the dipolar shifts (~1 kG for an Fe moment). On the other hand, for favorable Fe-alloy systems, linewidths of ~1.5 kG are attainable in pulsed NMR experiments. Thus the NMR technique is inherently better for observing the dipolar shifts.

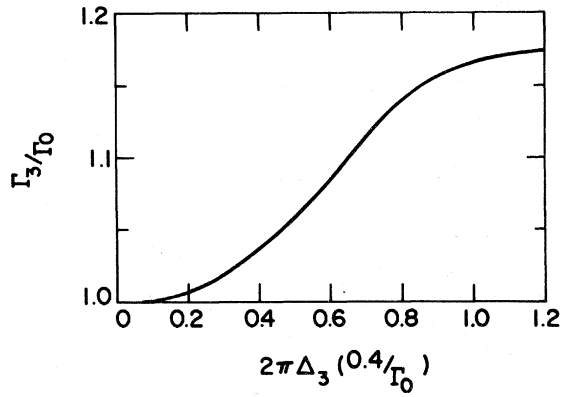

FIG. 7. Calculated ratios of $N3$ linewidth Γ_3 to main linewidth Γ_0 as a function of $N3$ dipolar shift. The linewidths are the full widths at half-height measured in MHz.

A most favorable alloy system in which to study dipolar shifts is in the nonstoichiometric alloys near Fe_3Si. Fe_3Si orders essentially perfectly, and there are three distinct well-separated NMR lines which can be observed[2]: A-type Fe atoms, which have 4-N1 Fe atoms and 4-N1 Si atoms, and D-type Fe atoms, which are surrounded by 8-N1 Fe atoms and Si atoms. The occupation of the first three neighbor shells for each of these species is given in Table I. Upon deviating from stoichiometry to the high-Fe side, the excess Fe atoms go randomly into the Si sites as D-type Fe atoms. The beauty of this system is that the NMR spectrum of each of these sites is sensitive to only one of the first three shells (also, only to two shells out of the first six). Thus, for example, in the spectrum for the D-type Fe atoms; the added Fe atoms give a

TABLE I. Number and type of neighbors for the three different sites in Fe_3Si.

Type	$N1$	$N2$	$N3$
A-Fe	4 D-4 Si	6 A	12 A
D-Fe	8 A	6 Si	12 D
Si	8 A	6 D	12 Si

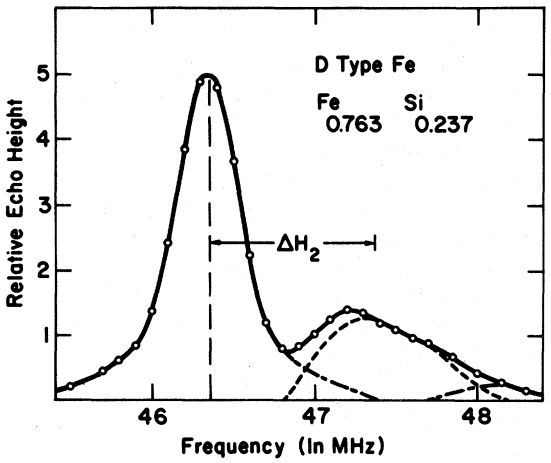

FIG. 9. Measured D-type Fe spectrum of an ordered $Fe_{0.763}Si_{0.237}$ alloy. The shift ΔH_2 is due to conduction-electron polarization from a D-type Fe atom in the second-neighbor shell. The dashed curve shows the dipolar broadening arising from one Fe atom in the second-neighbor shell.

satellite at a hyperfine field shift ΔH_2 corresponding to the conduction-electron polarization from an $N2$ D-type Fe atom, and this satellite has a shape determined by $N2$ dipolar shifts. Such a spectrum is shown in Fig. 9 for a 23.7-at.% Si alloy. The satellite has exactly the calculated intensity corresponding to its composition. We will see that the measured NMR dipolar shifts obtained for this system agree very well with the calculated dipolar shifts, thus indicating that the matrix distortions in either charge, spin, or geometry are small in this case.

Other alloys where the dipolar shifts are not directly measurable but should be considered[7] are those measured by Budnick *et al.*[8] These are alloys of Fe with the transition metals to the right of Fe in the periodic table, i.e., Co, Ni, Rh, Pd, and Pt. Although the turning angles were not measured in these experiments, we will assume that $\alpha_1 \sim 5$ rad, since that is the most likely operating condition for optimum spectra. For these alloys, it was observed[7] that when the solute atom moments differ appreciably from the host moment, the satellites have widths ~2.3 times greater than the main line. A $Fe_{0.968}Mo_{0.032}$ alloy was also observed to have an anomalous broadening[9] for the $N1$ and $N2$ neighbors of Mo. We will discuss how much broadening we expect due to dipolar shifts in these alloys. Of course there are other sources of broadening, e.g., distortion of the host band structure in the vicinity of the solute atom, loss of cubic symmetry around a solute atom due to the moment perturbations in the host moments, magnetic saturation effects,[2] and further distortion by impurity-impurities effects, especially in the more concentrated alloys. All of these effects are difficult to assess. It was observed in Ref. 7 that the broadening effects are even more pronounced in alloys with the 5d-transition-series elements.

A. $N1$ dipolar shifts

For the Fe_3Si system, the $N1$ broadening is best observed by comparing the linewidth of an A-type Fe atom with four D-type Fe's in the $N1$ shell ($\Gamma_0 = 0.59$ MHz) with the linewidth of an A-Fe atom with five D-type Fe's in the $N1$ shell ($\Gamma_1 = 0.75$ MHz). In both cases, there are 12 Si atoms in the $N4$ shell. All the data were taken with $\alpha_1 \simeq 5$ rad and $\alpha_2 \simeq 10$ rad.[2] In Fig. 4 we gave the calculated broadening due to a dipolar shift Δ_1. Using this curve, we obtain, from the observed broadening for the 23.7-at.% alloy, a value of $\Delta_1 = 0.20 \pm 0.03$ MHz. The calculated value is $\Delta_1 = 0.21 \pm 0.01$ MHz, where the D-Fe moment was measured in neutron experiments[10] to be $2.4 \pm 0.1 \mu_B$ and the lattice constant of Fe_3Si is 2.83 Å.[11] Thus the measured and calculated dipolar shifts for $N1$ are in excellent agreement, with no indication of any charge, spin, or lattice distortions. Cranshaw *et al.*[3(b)] obtained no net dipolar shift for the $N1$ effect in 4.9-, 6.1-, and 8.6-at.% Si alloys.

For the FeRh spectrum of Budnick *et al.*,[8] we obtained a value of $\mu_{Rh} = 1.1 \mu_B$. This gives a calculated value for Δ_1 of 0.09 MHz (0.7 kG). This would lead to an appreciable broadening of the $N1$ line, since $\Gamma_0 = 0.22$ MHz (1.6 kG). The $N1$ broadening is even greater for FePd, since the Pd moment is smaller. The broadenings needed to fit the data were about a factor 2.3; thus for the $N1$ case some but not all of this is attributable to dipolar broadening. In these alloys there is also a moment perturbation surrounding the solute atom. This will contribute additional broadening that is not included in the above estimate.

B. $N2$ dipolar shifts

The $N2$ broadening in the Fe_3Si system is observed by looking at the D-type Fe atoms. The spectrum of the D-Fe atoms for the 23.7-at.% alloy is shown in Fig. 9. Subtracting out the main line and a small contribution of 3% at the high-frequency end due to Fe atoms with two $N2$ Fe atoms, we obtain the dashed curve for the Fe atoms with only one Fe atom in the second shell. Since the Fe hyperfine field is negative, the shift caused by the conduction-electron polarization of the 4s electrons is seen to be negative, since it increases the hyperfine field. Thus a positive (negative) Δ_2 shift decreases (increases) the frequency, and the observed $N2$ line shape is therefore a reflection of the curves shown in Fig. 5. We find that the lineshape for $D = 1$ gives an excellent fit to the $N2$ line

shape in Fig. 9; $D = 0.9$ or 1.1 give poor fits. Taking into account the linewidth of the main line (0.48 MHz), we obtain $\Delta_2 = 0.19 \pm 0.04$ MHz (1.4 kG). A 22.95-at.% Si alloy also gave the same shifts. The calculated Δ_2 value is 0.14 ± 0.01 MHz (1 kG). Thus there is seen to be agreement between the measured and calculated $N2$ dipolar shift values again indicating little if any distortion in the Fe matrix. Cranshaw *et al.*[3] obtained a shift of[3(b)] 0.30 MHz for (5–9)-at.% Si alloys, but gave no estimation of the error.

For FeRh and FePd, the calculated Δ_2 shifts are 0.4 kG and 0.6 kG, respectively. This would lead to a D value of ~ 0.9 and thus a broadening with the skewed shape shown in Fig. 6 for $D = 1$. In this case the line shape is as shown because the moment is missing (as opposed to the Fe_3Si case, where it is added). Thus a broadening of a factor of ~ 1.3 could be due to $N2$ dipolar broadening in the FeRh and FePd spectra,[7] but it was observed that about a factor of 2.3 was needed to fit the spectra. So there must also be other sources of broadening. Again, one source is that due to the perturbed moments in the Fe matrix.

C. $N3$ dipolar shifts

The $N3$ broadening in the Fe_3Si system would show up as a broadening of the Si spectrum for those Si atoms with a D-type Fe atom in the $N3$ shell of Si(1 Fe, $N3$) in comparison to the Si spectrum of those which have only Si atoms in the $N3$ shell Si(0 Fe, $N3$). Unfortunately, the A-type Fe lines overlap with these Si(1 Fe, $N3$) lines; so an accurate determination of Δ_3 is impossible. However, for the 23.7-at.%-Si alloy the Si(1 Fe, $N3$) linewidth did appear to be broader than the Si(0 Fe, $N3$) linewidth by about a factor of 1.1. From Fig. 8, this would lead to a measured $\Delta_3 \simeq 0.14$ MHz ($\Gamma_0 \simeq 0.59$ MHz). The calculated value for $\Delta_3 = 0.05$ MHz (or 0.35 kG). Considering the large uncertainties in the measured linewidth of Si(1 Fe, $N3$), the Δ_3 value is considered to be consistent with the calculated value.

For the FePd alloy[7,8] we calculate $\Delta_3 \sim 0.2$ kG, which corresponds to a $D \simeq 0.3$. Thus there should be no appreciable dipolar broadening of $N3$ Fe neighbors to a Pd atom due to loss of moment. Since the $N3$ satellite is the most prominent one in these alloys, the observed broadening of the satellites in the FePd and FeRh alloys must be mainly due to effects other than the dipolar broadening due to loss of moment at the solute atom.

IV. CONCLUSIONS

Calculation of the dipolar broadenings due to loss of cubic symmetry near a solute atom in a domain wall has been made for the first three neighbor shells. We find that the shape of the lines due to dipolar shifts depends very much on turning angles, and we discuss optimum operating conditions for measuring the dipolar shifts.

We then obtain the dipolar shifts for the $N1$ and $N2$ shells of ordered FeSi alloys. We find that for this system the measured dipolar shifts are in agreement with the calculated values. This indicates that in this system there are negligible charge, spin, or geometric distortions on replacing a Si atom with an Fe atom. The dipolar shifts in dilute FeRh and FePd systems are also estimated, and it is found that the "anomalous" broadening of the satellite lines needed to reproduce these alloy spectra cannot be accounted for by a simple dipolar broadening due to the loss of moment on the solute atom.

[1] G. A. Murray and W. Marshall, Proc. Phys. Soc. 86, 315 (1965); referred to as MM.

[2] M. B. Stearns, Phys. Rev. B 4, 4069 and 4081 (1971).

[3] (a) T. E. Cranshaw, C. E. Johnson, and M. S. Ridout, in *Proceedings of the International Conference on Magnetism* (Institute of Physics and Physical Society, London, 1964), p. 141; (b) T. E. Cranshaw, C. E. Johnson, and M. S. Ridout, Phys. Lett. 21, 481 (1966).

[4] E. Lifshitz, J. Phys. USSR 8, 337 (1944); L. Néel, Cahiers Phys. 25, 1 (1944); see also C. Kittel and J. K. Galt in *Solid State Physics*, edited by F. Seitz and D. Turnbull (Academic, New York, 1967), Vol. 3, p. 437.

[5] M. B. Stearns, Phys. Rev. 162, 496 (1967); 187, 648 (1969); M. B. Stearns and J. F. Ullrich, Phys. Rev. B 4, 3825 (1971).

[6] M. B. Stearns, AIP Conf. Proc. 10, 27 (1973).

[7] M. B. Stearns, Phys. Rev. B 9, 2311 (1974).

[8] J. I. Budnick, T. J. Burch, S. Skalski, and K. Raj, Phys. Rev. Lett. 24, 511 (1970).

[9] A. Asano and L. H. Schwartz, AIP Conf. Proc. 18, 262 (1974).

[10] A. Paoletti and L. Passari, Nuovo Cimento 32, 25 (1964).

[11] W. B. Pierson, *A Handbook of Lattice Spacing* (Pergamon, New York, 1958).